Progress In Electromagnetics Research Letters, Vol. 94, 157–163, 2020

Design and Construction of a Nonuniform Wiggly Lines Bidirectional Coupler in Combination with the Reflected Power Canceller Method

Pouya Mehrjouseresht*, Mahshad Rezvani, Majid M. Demneh, and Reza Motahari

Abstract—This paper presents a bidirectional coupler which is designed by combining nonuniform wiggly lines and the reflected power canceller (RPC) method. The combination not only brings about a high directivity but also makes a wideband structure with a compact size. Although, in the RPC method, an idle port is used to produce a reflected signal in order to achieve a high directivity, there are not any idle ports in the proposed coupler. The coupler was built on an FR4 substrate. The measurement results show that this structure is suitable to monitor forward and reflected signals in high power applications. The fabricated coupler has the directivity of more than 22 dB and the coupling flatness of ± 0.12 dB in the forward and backward signals in a wide frequency range of 140 MHz–190 MHz.

1. INTRODUCTION

Couplers are essential components to sample forward and reflected powers in different RF/microwave systems. Wideband bidirectional couplers, which have a compact size, play a pivotal role in power monitoring systems operating in the VHF band. Also, in the case of high power signals, bidirectional couplers should have weak coupling with flat response because power detectors are low-power devices and have good performance for a certain range of input power level. Furthermore, the monitoring cannot be accurately done when there is not isolation between the forward and reflected signals. Therefore, the couplers should have not only the weak coupling but also high directivity. Among different coupler structures, microstrip couplers are very common since they are easily fabricated and integrated with other structures, but they suffer from poor directivity. There are different techniques to achieve high directivity couplers with a wide frequency band and compact size. Methods such as inductive compensation [1], delay lines [2], wiggly lines [3, 4], and the reflected power canceller [5] are some techniques to enhance directivity. To increase couplers bandwidth, using nonuniform lines, dielectric overlay [6], and changing geometry of couplers [7] are some useful methods. Reducing the size of couplers involves methods such as employing lumped elements on output ports [8], or applying stubs, folded structures, and a slotted ground plane [9–11]. The couplers can be achieved by combining some of the aforementioned techniques. In the VHF band, lumped elements are commonly utilized in various designs, for they introduce a degree of freedom in tuning. As a result, the methods including lumped elements are appropriate candidates.

In this paper, the reflected power canceller (RPC) method and nonuniform wiggly lines are employed to implement a high directivity and wideband bidirectional coupler operating in the VHF band. The nonuniform wiggly lines improve the directivity and bandwidth while the RPC method plays a pivotal role in acquiring a coupler with higher directivity. To reduce the size of the coupler, capacitors on the sampling ports are suggested. This coupler is suitable for sampling forward and reflected high power

Received 17 August 2020, Accepted 10 November 2020, Scheduled 18 November 2020
* Corresponding author: Pouya Mehrjouseresht (p.mehrjooseresht@alumni.iut.ac.ir).
The authors are with the Department of Electrical and Computer Engineering, Isfahan University of Technology, Isfahan, Iran.

signals. Another important advantage of this design is that there is not idle port which is used to enhance directivity in the RPC method. Consequently, all ports of the coupler are utilizable, and the bidirectional coupler can be realized.

2. THEORY

The schematic diagram of the proposed coupler is shown in Fig. 1. Port 3 samples the forward signal, and port 4 samples the reflected signal. To understand how the coupler combined with the RPC method operates, there is a diagram in Fig. 2(a) with colored lines, which show the signal paths. In the reflected power canceller method, the idle port is considered to make an intended mismatch and remove the

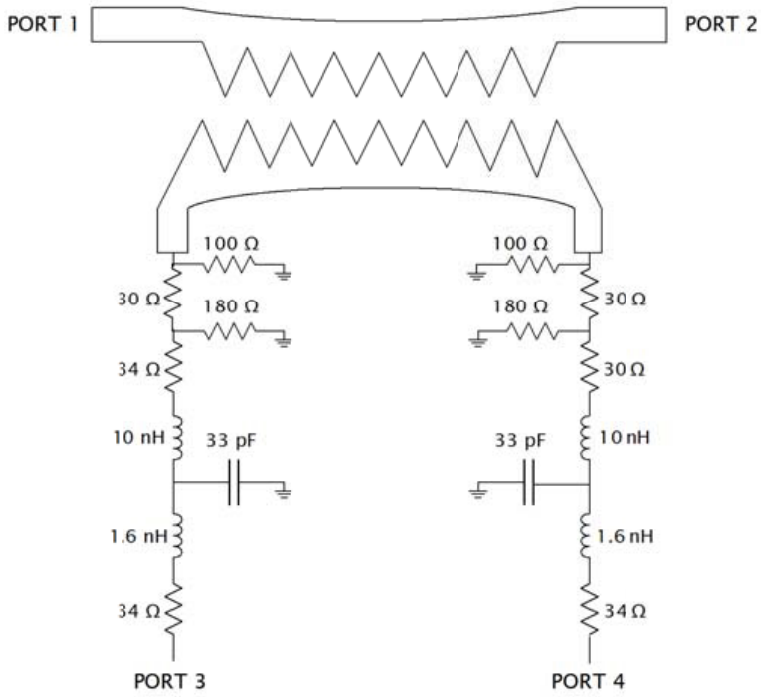

Figure 1. Schematic diagram of the proposed coupler.

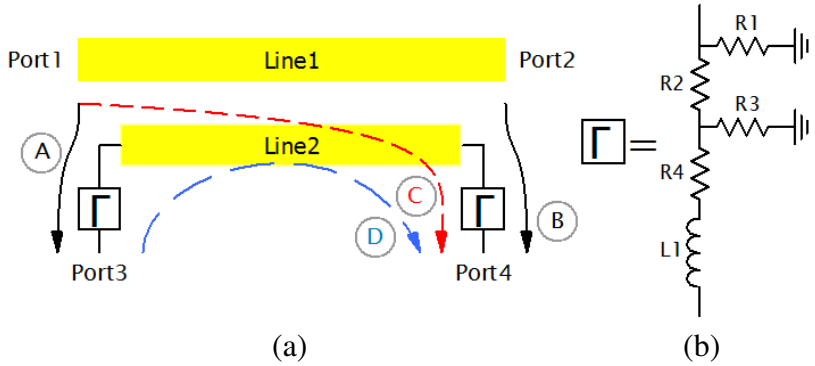

Figure 2. (a) Signal paths in the proposed coupler, there are signals similar to C and D at port 3 too, (b) the suggested Γ circuit.

signal which has the same magnitude and anti-phase of the leakage reflected signal to the sampling port. In Fig. 2(a), the intended mismatch is generated by Γ on port 4 and port 3. Consequently, there is not idle port which is employed in the typical RPC method. As seen from Fig. 2(a), the mismatch on port 3 creates signal D on port 4, and an incident signal at port 1 is divided into signal A, which is the sampled forward signal at port 3, and signal C, which is the leakage signal from port 1 at port 4. Also, the sampled backward signal at port 4 is signal B. To have high directivity at port 4, signals C and D must be canceled out by designing the Γ circuit properly. This explanation is also given for port 3. The proposed Γ circuit making the mismatch is shown in Fig. 2(b).

Signals $A,\ B,\ C$, and D can be described by $ABCD$ matrix [5]. This matrix is equal to the $ABCD$ matrix of Γ circuit in Eq. (1) for signals A and B, and is obtained by multiplying the $ABCD$ matrix of each cascade component in a signal path for signals C and D in Eq. (2).

$$\begin{bmatrix} A_\Gamma & B_\Gamma \\ C_\Gamma & D_\Gamma \end{bmatrix} = \begin{bmatrix} 1+\dfrac{R_3}{R_2} & (R_4+j\omega L_1)\left(1+\dfrac{R_3}{R_2}\right)+R_3 \\ \dfrac{R_1+R_2+R_3}{R_1R_2} & (R_4+j\omega L_1)\left(\dfrac{R_1+R_2+R_3}{R_1R_2}\right)+\left(1+\dfrac{R_3}{R_1}\right) \end{bmatrix} \tag{1}$$

$$\begin{aligned} \begin{bmatrix} A_C & B_C \\ C_C & D_C \end{bmatrix} &= \begin{bmatrix} A_{TL} & B_{TL} \\ C_{TL} & D_{TL} \end{bmatrix} \begin{bmatrix} A_\Gamma & B_\Gamma \\ C_\Gamma & D_\Gamma \end{bmatrix}, \\ \begin{bmatrix} A_D & B_D \\ C_D & D_D \end{bmatrix} &= \begin{bmatrix} A_\Gamma & B_\Gamma \\ C_\Gamma & D_\Gamma \end{bmatrix} \begin{bmatrix} A_{TL} & B_{TL} \\ C_{TL} & D_{TL} \end{bmatrix} \begin{bmatrix} A_\Gamma & B_\Gamma \\ C_\Gamma & D_\Gamma \end{bmatrix} \end{aligned} \tag{2}$$

where the matrix of TL is the $ABCD$ matrix of the transmission line given in [5]. By deriving scattering matrices from Eqs. (1) and (2), and the condition $\text{Signal}\,C + \text{Signal}\,D = 0$ to have high directivity at port 4, we find

$$S_{21}^D a_1^D + S_{21}^C a_1^C = 0 \tag{3}$$

If the reflected wave coefficients b_2^A and b_2^B are equal, it can be obtained that the incident wave coefficient a_2^A is equal to $\frac{S_{21}^A}{S_{22}^A} a_1^B$. By using Eq. (3) and assuming $a_2^A = a_1^D$ and $a_1^B = -a_1^C$, we have

$$S_{21}^D \times S_{21}^A = S_{22}^A \times S_{21}^C \tag{4}$$

where

$$\begin{aligned} S_{21}^A &= \frac{2}{A_\Gamma + D_\Gamma + Z_0 C_\Gamma + \dfrac{B_\Gamma}{Z_0}} \\ S_{22}^A &= \frac{-(A_\Gamma - D_\Gamma) - Z_0 C_\Gamma + \dfrac{B_\Gamma}{Z_0}}{A_\Gamma + D_\Gamma + Z_0 C_\Gamma + \dfrac{B_\Gamma}{Z_0}} \\ S_{21}^C &= \frac{2}{\left(A_\Gamma + D_\Gamma + Z_0 C_\Gamma + \dfrac{B_\Gamma}{Z_0}\right)(\cos\beta d + j\sin\beta d)} \\ S_{21}^D &= \frac{2}{(M\cos\beta d + jN\sin\beta d)} \\ M &= (A_\Gamma)^2 + (D_\Gamma)^2 + 2B_\Gamma C_\Gamma + (A_\Gamma + D_\Gamma)\left(Z_0 C_\Gamma + \frac{B_\Gamma}{Z_0}\right) \\ N &= \left(\frac{B_\Gamma}{Z_0}\right)^2 + (Z_0 C_\Gamma)^2 + 2A_\Gamma D_\Gamma + (A_\Gamma + D_\Gamma)\left(Z_0 C_\Gamma + \frac{B_\Gamma}{Z_0}\right) \end{aligned}$$

In Eq. (4), Z_0 and d are the characteristic impedance and the physical length of line 2, respectively.

3. DESIGN OF THE PROPOSED COUPLER

The nonuniform wiggly coupled lines are designed employing formulas given in [12, 13]. First, the familiar Equation (5) is optimized for a range of spacing between conductors from 0.015 mm to 18 mm, dielectric constant of 4.8, substrate thickness of 2.4 mm, $Z_0 = 50\,\Omega$, $f_1 = 140$ MHz, and $f_2 = 190$ MHz to obtain width of strips.

$$Z_0^2 c^2 C_e^a C_o^a \sqrt{\varepsilon_{re}^e(f)\varepsilon_{re}^o(f)} - 1 = 0 \tag{5}$$

where Z_0 and c are the characteristic impedance and velocity of light in vacuum, respectively. ε_{re}^e and ε_{re}^o are effective dielectric constants for the even and odd modes, respectively, and $C_{e,o}^a$ is the even and odd mode capacitance for the coupled microstrip line configuration with air as dielectric [12]. After computing even and odd mode characteristic impedances, even and odd mode effective dielectric constants, wiggle depth, and voltage coupling coefficient [12, 13], continuous coupling coefficient is obtained by using Eq. (6) and coupling of 15 dB [13].

$$k\,(x) = \frac{Z_{0e}^2\,(x) - 1}{Z_{0e}^2(x) + 1} \tag{6}$$

where $Z_{0e}(x)$ is the normalized even mode impedance [13]. Finally, the width of strips, the spacing between lines, and the wiggle depth along the coupler length can be formed by evaluating the conductor width, conductor spacing, and wiggle depth versus the voltage coupling coefficient, respectively, at all values of $k(x)$ [13]. The physical parameters are shown in Fig. 3. As seen, the whole length of the wiggly coupled line is 41.48 mm, and the line spacing and wiggle depth vary from 10.23 to 7.61 mm and 5.5 to 4.97 mm, respectively. In addition, the line width changes from 4.35 mm to 4.34 mm. To shrink the structure, the capacitor is placed parallel with Γ circuit. This capacitor and elements of Γ circuit affect the performance of the coupler and are defined by ADS simulation (Keysight Technology) and tuned to meet the coupling factor of 55–60 dB with 0.2 dB flatness and the directivity more than 20 dB. The obtained values of Γ at port 3 and the capacitor are equal to $R_1 = 100\,\Omega$, $R_2 = 30\,\Omega$, $R_3 = 180\,\Omega$, $R_4 = 34\,\Omega$, $L_1 = 10$ nH and $C = 33$ pF, respectively. The element values of Γ at port 4 are similar to Γ at port 3 with $R_4 = 30\,\Omega$. As seen in Fig. 1, there is an inductor in series with a resistor, which matches the impedances of port 3 and port 4 to the input impedance of the power detectors. It is striking that they have no influence on the performance of the coupler. For the 50 Ω input impedance, the resistor and inductor are 34 Ω and 1.6 nH, respectively.

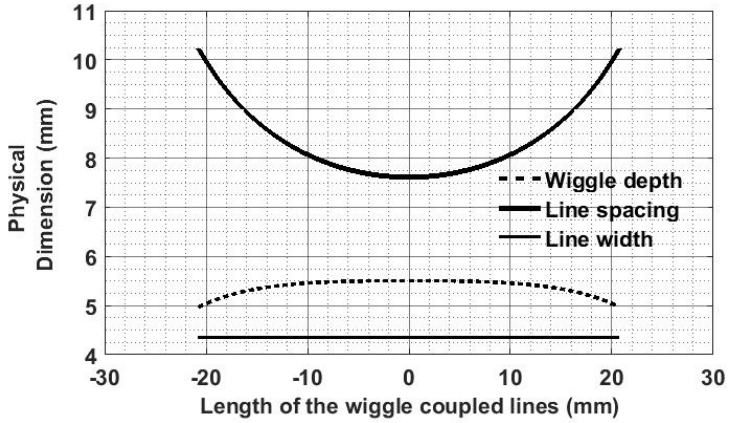

Figure 3. Variations of the physical geometry along the wiggly coupled lines length.

4. SIMULATION AND MEASUREMENT RESULTS

Figure 4 illustrates the proposed coupler built on FR4 with relative permittivity 4.8 and substrate thickness 2.4 mm. The measured and simulated S parameters are shown in Fig. 5 to Fig. 7. All

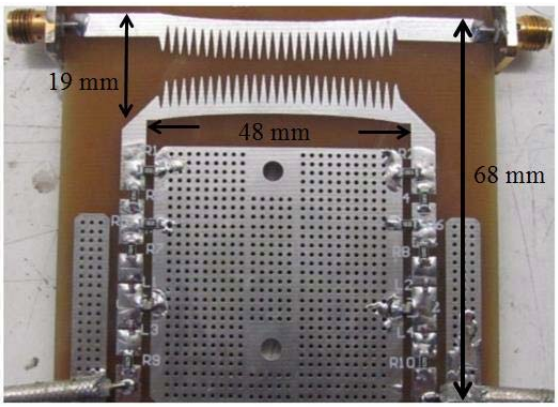

Figure 4. The fabricated proposed coupler.

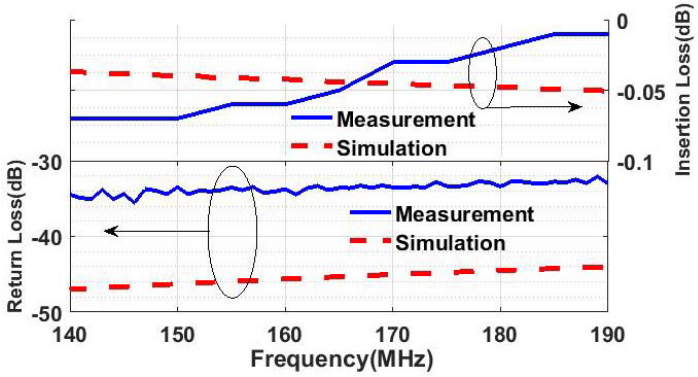

Figure 5. Measured and simulated insertion and return loss.

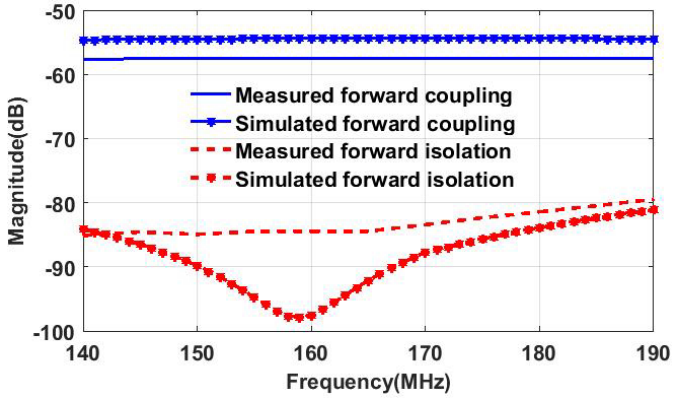

Figure 6. Measured and simulated forward coupling and isolation.

simulations were performed with Keysight ADS Momentum. In Fig. 5, the measured insertion and return loss are better than -0.1 dB and -30 dB, respectively. Also, the forward and backward couplings and isolations are seen in Fig. 6 and Fig. 7, respectively. Since the directivity is high within the operational bandwidth, it is very sensitive to fabrication and substrate tolerances. Therefore, there is a difference between simulation and measurement results in the isolation. As seen, the measured directivity is more than 22 dB from 140 MHz to 190 MHz in the forward and backward direction. The measured coupling is close to the simulated value, and it is -57.53 ± 0.1 dB for the forward signal and -57.22 ± 0.12 dB

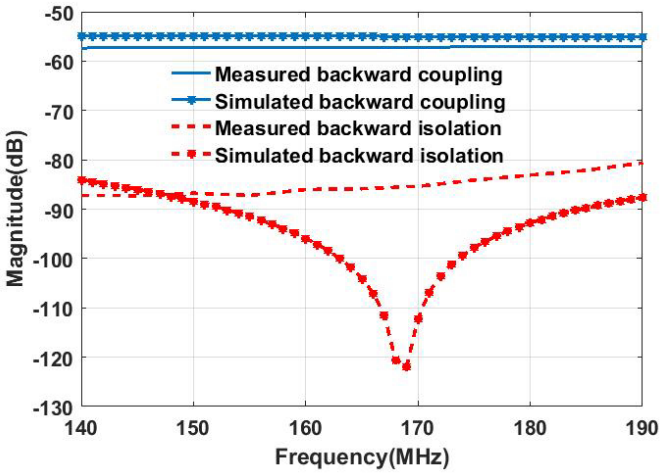

Figure 7. Measured and simulated backward coupling and isolation.

for the backward signal. Consequently, the coupling value is within a suitable range in order to sample high power signals (≈ 60 dBm) in power monitoring systems. It is worth mentioning that port 3 and port 4 have the same coupling value, and there are not any idle ports although the RPC method is employed.

5. CONCLUSION

In this paper, the reflected power canceller method and nonuniform wiggly lines are employed to realize a bidirectional coupler which is used to sample the forward and reflected signals in power monitoring systems. One of the positive points of the proposed coupler is that there is not idle port used in the typical RPC method. Moreover, high directivity and fine coupling flatness in a wide frequency band (140 MHz–190 MHz) and a compact size are some other advantages. Since the sampled signals are applied to power detectors, which are low-power devices, having a weak coupling is important. The measured results show that the coupling value is -57.53 ± 0.1 dB and -57.22 ± 0.12 dB for the forward and backward directions, respectively, which are suitable values in high power monitoring systems. In addition, the directivity is more than 22 dB for both directions within the operational band.

REFERENCES

1. Lee, S. and Y. Lee, "An inductor-loaded microstrip directional coupler for directivity enhancement," *IEEE Microwave and Wireless Components Letters*, Vol. 19, No. 6, 362–364, Jun. 2009.
2. Chun, Y., J. Moon, S. Yun, and J. Rhee, "Microstrip line directional couplers with high directivity," *Electronics Letters*, Vol. 40, No. 5, 317–318, March 4, 2004.
3. Moscoso-Martir, A., I. Molina-Fernandez, and A. Ortega-Monux, "High performance multi-section corrugated slot-coupled directional couplers," *Progress In Electromagnetics Research*, Vol. 134, 437–454, 2013.
4. Hrobak, M., M. Sterns, E. Seler, M. Schramm, and L. Schmidt, "Design and construction of an ultrawideband backward wave directional coupler," *IET Microwaves, Antennas & Propagation*, Vol. 6, No. 9, 1048–1055, June 19, 2012.
5. Sohn, S., A. Gopinath, and J. T. Vaughan, "A compact, high power capable, and tunable high directivity microstrip coupler," *IEEE Transactions on Microwave Theory and Techniques*, Vol. 64, No. 10, 3217–3223, Oct. 2016.
6. Peláez-Pérez, A. M., P. Almorox-Gonzalez, J. I. Alonso, and J. González-Martín, "Ultra-broadband directional couplers using microstrip with dielectric overlay in millimeter-wave band," *Progress In Electromagnetics Research*, Vol. 117, 495–509, 2011.

7. Yıldırım, B. S. and K. Karayahşi, "Broadband UHF microstrip coupler," *AEU-International Journal of Electronics and Communications*, Vol. 108, 2019.
8. Maloratsky, L. G., *Passive RF & Microwave Integrated Circuits*, Elsevier/Newnes, Amsterdam, 2004.
9. Singh, S., R. P. Yadav, and A. Jain, "Miniaturized dual-band branch-line coupler with folded stubs," *2019 IEEE 5th International Conference for Convergence in Technology (I2CT)*, Bombay, India, 2019.
10. Coromina, J., P. Vélez, J. Bonache, and F. Martín, "Branch line couplers with small size and harmonic suppression based on non-periodic step impedance shunt stub (SISS) loaded lines," *IEEE Access*, Vol. 8, 67310–67320, 2020.
11. Liu, G.-Q., L.-S. Wu, and W.-Y. Yin, "A compact microstrip rat-race coupler with modified lange and T-shaped arms," *Progress In Electromagnetics Research*, Vol. 115, 509–523, 2011.
12. Kirschning, M. and R. H. Jansen, "Accurate wide-range design equations for the frequency-dependent characteristic of parallel coupled microstrip lines," *IEEE Transactions on Microwave Theory and Techniques*, Vol. 32, No. 1, 83–90, Jan. 1984.
13. Uysal, S., *Nonuniform Line Microstrip Directional Couplers and Filters*, Artech House, 1993.